2020-09

Preparation of supporting photocatalysts for water treatment using natural sunlight as an alternative driving energy

Harikaranahalli Puttaiah, S

10.1016/j.matpr.2020.08.020
Materials Today: Proceedings
Elsevier

Materials Today: Proceedings xxx (xxxx) xxx

Contents lists available at ScienceDirect

Materials Today: Proceedings

journal homepage: www.elsevier.com/locate/matpr

Preparation of supporting photocatalysts for water treatment using natural sunlight as an alternative driving energy

Harikaranahalli Puttaiah Shivaraju [a,b,*], Menon Saparsha [a], Shivamurthy Ravindra Yashas [a], Kumari Sonu [a], Revanna Harini [b], David Jenkins [c]

[a] Division of Environmental Science, Department of Water and Health, JSS Academy of Higher Education and Research, Mysuru 570015, India
[b] Center for Water, Food and Energy, The GREENS Trust, Harikaranahalli, Dombaranahalli Post, Turuvekere Taluka, Tumkuru 572215, India
[c] Wolfson Nanomaterials & Devices Laboratory, School of Computing, Electronics and Mathematics, Faculty of Science & Engineering, University of Plymouth, Devon PL4 8AA, UK

ARTICLE INFO

Article history:
Received 18 February 2020
Accepted 3 August 2020
Available online xxxx

Keywords:
Titanium dioxide
Photocatalysis
Sunlight
F-TiO_2
Si-TiO_2

ABSTRACT

The present study focus on synthesis of visible-light active pure, Fluoride (F) - and Silica (Si)-doped titanium dioxide (TiO_2) photocatalyst. Designing the nanoparticles under sol–gel process of synthesis method is adopted. Characterizations such as SEM, XRD, FTIR, and DLS revealed about the crystallinity, physico-catalytic properties of the photocatalysts. The nanomaterials were tested for their photocatalytic properties against crystal violet, methyl orange, oil and grease and chemical oxygen demand (COD) remediation. To check the degradation efficiency samples were kept in different light sources namely natural sunlight, dark + sunlight and LED light and were tested using UV–Vis spectroscopy. It is noteworthy that the as-synthesized materials best acted on target parameters under natural sunlight (visible range) which a renewable sources of energy taken as an alternative driving energy. Specifically, Si-doped TiO_2 was found to be superior over F-doped and pure (undoped) TiO_2 in terms of degradation efficiencies.

Selection and Peer-review under responsibility of the scientific committee of the 2nd International Conference on Nanoscience and Nanotechnology.

1. Introduction

With the growing population, development in industrialization and urbanization is taking place at a faster rate which not only bringing the comfort in lifestyle but it also making it more problematic at the same time [1]. Among all pollution, treatment of water pollutants are gaining more attention of scientists and researchers as water is the basic of man daily work from a household need to a raw material for industries [2]. Instead of having too many water treatment processes, treatment of water is a costly procedure and to solve this new sustainable technologies are brought into the field of wastewater treatment [3]. Heterogeneous photocatalysis for water treatment has been reviewed profoundly in discrete perspectives for an environmental application [4]. TiO_2 were used extensively as a photocatalyst for the degradation of organic pollutants in the water and wastewater as it is cost-effective, non-toxic, chemically stable, highly resistance to photodegradation [5–13]. As TiO_2 is known to be the most appropriate photocatalyst but the direct dispersion of TiO_2 nanoparticles in larger amount may have some disadvantage such as the powder may sink or suspends in the solution which interrupt in the light penetration, then problem of agglomeration, as the size of the nanoparticles are so small ranges between (30–300 μm) which are not recovered hence it does not allow it to reuse for next [14–16]. To overcome such issues, several new techniques are coming into existence such as incorporation of nanopowder into or onto the membrane, coating onto the beads etc. Coating of nanoparticles on floating beads has gained more attention recently as it utilizes the maximum sunlight for the reaction to be happened [17]. Floating beads need to be prepared in a way that it should on or near the water surface for enough period of time and the nanocatalyst present on the surface should get enough time to accelerate the photocatalytic reaction upon sunlight irradiance. Making beads to float several criteria needs to be kept in mind i.e. density of beads should be less than water density, it has a good cohesion support, should be unreactive with nanoparticles, beads should be hydrophobic so that it would not dissolve upon coming in contact with water, the dimension of the beads should be small enough to retard the precipitation process [15].

* Corresponding author.
E-mail address: shivarajuenvi@gmail.com (S. Harikaranahalli Puttaiah).

https://doi.org/10.1016/j.matpr.2020.08.020
2214-7853/
Selection and Peer-review under responsibility of the scientific committee of the 2nd International Conference on Nanoscience and Nanotechnology.

Hence, the purpose of the present study is to prepare and characterize visible–light responsive supported photocatalytic nanoparticles and to enhance the photocatalytic degradation efficiency of commercial dyes and oil and grease in wastewater using pure TiO_2, Si-TiO_2 and F-TiO_2 nanopowders under natural sunlight radiated as an alternative source of energy. In addition, wastewater treatment using supported photocatalytic nanomaterials under visible light sources was demonstrated and an easy way of recovery of suspended photocatalytic nanoparticles from aqueous media using proper supporting materials was made possible which decreases the operation cost and intensify the radiance efficiency which can be reused.

2. Materials and methods

2.1. Sol-gel preparation of pure TiO_2, F-doped TiO_2 and SiO_2-doped TiO_2

Preparation of pure TiO_2 photocatalyst was carried out under the process of sol–gel in which titanium tetra isopropoxide (TTIP) is taken as a pioneer precursor. In order to prepare pure TiO_2, 15 ml TTIP (Spectrochem, Pvt. Ltd, India) of 98% purity was taken and added to100 ml isopropyl alcohol in an 250 ml of volumetric flask and the mixture stirred for 10 min on the magnetic stirrer constantly at 500 rpm followed by the addition of 10 ml of cold water drop-wise. At a room temperature, the resultant compound was continuously stirred at 500 rpm for 12 h followed by aging by keeping the samples in a dark box for 24 h with no any external hindrance. Afterwards, the aqueous compound of pure TiO_2 was washed frequently with deionized water and dehydrated in a dust-free hot air oven at 55 °C. The obtained powder was then kept in a dust-free muffle furnace using a silica vessel provided with lid at 600 °C for 2 h in order to enhance stability of the materials and also to ensure elimination of trace pollutants. Finally, it was grinded into powder at room temperature to get aimed crystallinity and active surface morphology and then transferred into air-tight sample tubes. Fig. 1 represents the schematic preparation of pure TiO_2, F-doped TiO_2, Si-doped TiO_2 nanoparticles through sol–gel technique. The samples were prepared in three replicate form among which, one remains in the pure form, the other two TiO_2 solutions are used for doping of non-metals. The two dopants

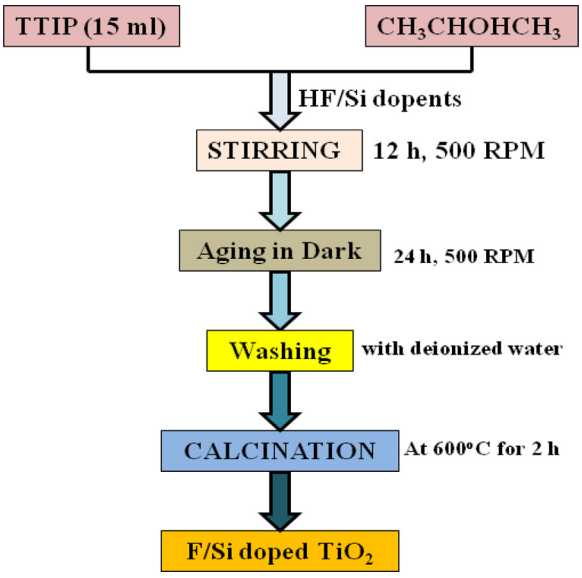

Fig. 1. Schematic of photocatalytic nanomaterials preparation under sol–gel technique.

includes firstly, F-doped TiO_2 was prepared by preparing the fluoride solution by adding 0.5 ml of Hydrogen Fluoride (HF) in 50 ml of double distilled water. From this solution, 10 ml of solution was added drop-wise to the TTIP dissolved in isopropyl alcohol and secondly, Si-doped 0.1g of Silica gel was dissolved in about 3 ml of acetic acid as it is insoluble in water. After dissolution, it was made up to 10 ml with double distilled water and added to the TTIP dissolved in isopropyl alcohol, drop-wise.

2.2. Characterization

As-synthesized photocatalytic materials (pure TiO_2, F-doped TiO_2, Si-doped TiO_2 nanoparticles) were subjected to numerous characterisation techniques to obtain information about their absorption band shifting, crystal size, surface morphology, photocatalytic activity, etc. The following analytical techniques and instruments were employed for this purpose are UV–Visible spectroscopy (Shimadzu UV-2100) to identify the highest peak and to monitor the dye degradation efficiency, the percentage of transmission. Powder X-ray diffraction (XRD) to determine the atomic and molecular structure of a crystal, Zeta sizer for dynamic light scattering (DLS) to obtain the particle size of prepared nanomaterials, Fourier transform infrared spectroscopy (FTIR) (Shimadzu-8400S) to analyze the presence of functional groups and Scanning electron microscopy (SEM) to analyze the surface morphology and cross-section of nanoparticles.

2.3. Preparation of supported photocatalysts

Bentonite clay is a very good adsorbent. By modifying it, many of its inherent and acquired properties can be enhanced to a greater degree. Clay does not contribute to additional toxicity in the water and hence is a viable supporting material. For the preparation of the hollow clay spheres, 25 g of Bentonite clay was taken, along with 4 g of Cellulose powder and 1 g of Ferric oxide. 1% Sodium lauryl sulphate solution was prepared and used to combine the above ingredients to form malleable dough. The secondary stage of preparation involved selection of suitable thermocol (a type of expanded polystyrene foam) beads, upon which a thin layer of the prepared clay was moulded. These clay beads were left to air dry overnight. Pure TiO_2, F-doped TiO_2 and Si-doped TiO_2 were coated on top of these clay spheres the following day and then placed in a muffle furnace that reached 600 °C for a period of 4 h. Thermocol melted within the clay at temperatures close to 210–250 °C and clay developed sturdy mechanical strength after this sintering process depicted in Fig. 2. In this manner, the clay spheres were rendered hollow using an inexpensive technique involving the thermocol.

2.4. Treatment of dyes and pollutants in water

Photocatalytic of modeled dyes were carried out by exposing the as per prepared samples of crystal violet and methyl orange to the natural sunlight of visible range, LED light and the one in dark prior to visible light exposure for 2 hrs and then placed in sunlight. The reason behind doing this is to test the adsorption capabilities of the clay prior to photodegradation. Both dye samples was prepared in 50 ml of distilled water of 0.01 M and 15 mg of composites. In this photocatalytic experiment, 50 ml of prepared dye solution in 100 ml of beaker was taken and the beads coated with Pure TiO_2, F-doped TiO_2 and Si-doped TiO_2 were added to it and then placed under natural sunlight, LED light and in dark for the same time interval. Complete set of experiments were done for 5 hrs of irradiation under natural sunlight (11 am to 4 pm), LED and dark without any interruption. The photodegradation efficiency was analyzed after each hour using double-beam UV–Vis

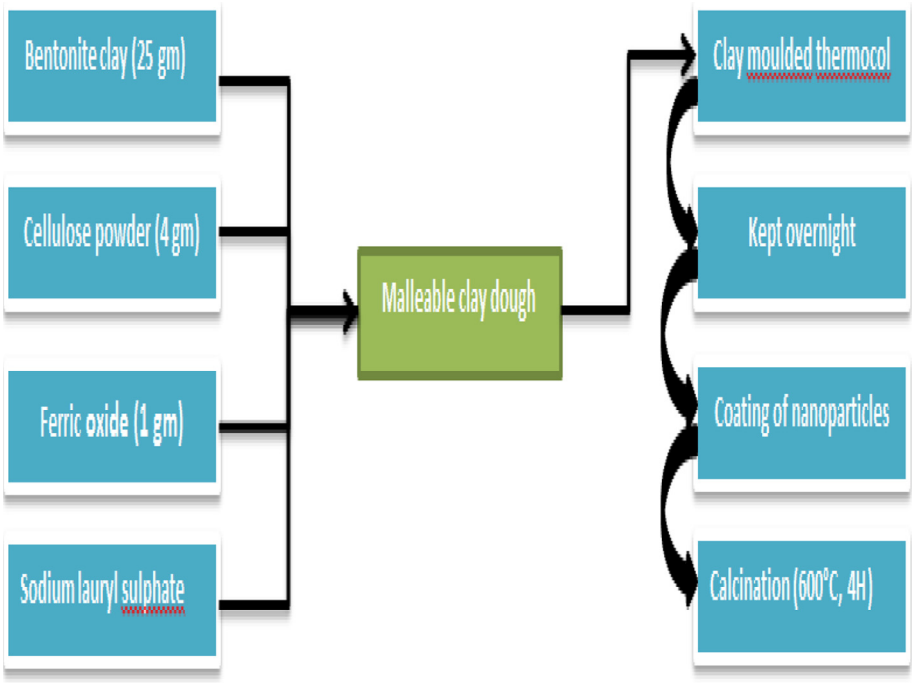

Fig. 2. Schematic representation of clay beads preparation procedure.

spectrophotometer at 590 nm (SHIMADZU (UV-1800)). Municipal sewage wastewater was collected from the sewage treatment plant located in the area of Kesare in Mysore district, Karnataka in order to determine the oil and grease and COD by using Partition-gravimetric and titrimetric method respectively. The samples were subjected to photodegradation up to 6 h and were analyzed for every 2 hrs. The rate of removal of oil and grease and COD were calculated using Eqs. (1) and (2):

$$\text{Oil and grease (mg/l)} = ((A - B) * 1000)/(\text{volume of sample}) \quad (1)$$

where, A and B are the final and initial weight of the beaker in gram.

$$\text{COD (mg/l)} = ((B - S) * \text{FAS(N)} * 8 * 1000)/(\text{volume of sample}) \quad (2)$$

where, B and S are the volume of FAS used for blank and sample respectively.

3. Results and discussions

3.1. Characterization and uniqueness

The photocatalytic materials Pure TiO_2, F-doped TiO_2 and Si-doped TiO_2 were prepared by sol-gel technique and were characterized using suitable analytic techniques such as DLS, UV–Vis spectroscopy, XRD, FTIR, SEM and photocatalytic activity. The size of the composites was measured by the DLS technique using Zetasizer instrument. Results obtained from DLS analysis of the as-prepared materials are shown in Fig. 3 and the results of each nanoparticle were revealed TiO_2 (352.4 nm), Si-doped TiO_2 (396.2 nm) and F-doped TiO_2 (1046.8 nm). Characterising the shifting of bandgap energy for pure TiO_2, F-doped TiO_2 and Si-doped TiO_2 nanomaterials were measured via UV–Vis spectrophotometer and the obtained results were compared with pure TiO_2. The UV–Vis absorption spectrum of pure TiO_2, F-doped TiO_2 and Si-doped TiO_2 polyscales are depicted in Fig. 4. It was found that bandgap energy of 2.96, 3.06 and 3.13 eV was observed for Si-TiO_2, F-TiO_2 and TiO_2 respectively falling in the range of visible spectrum of light.

To determine the functional groups and to study the vibrational motion of atoms and molecules FTIR spectroscopy is used [18]. In this, each molecule absorbs only IR light of certain frequencies based on the molecule characteristics which makes it possible to identify the type of molecule known as qualitative analysis and the amount of molecules in the sample simply called the quantitative analysis by analyzing the absorption spectrum. The FTIR spectra of the samples of different composition are shown in Fig. 5. As it is shown in figure, the spectra show certain significant absorption peaks observed in the range of 4000 to 400 cm^{-1}. The absorption peak observed at 2000–3400 cm^{-1} is accredited to OH stretching vibrations of H_2O in the TiO_2 compound, while absorption band at 1637 cm^{-1} harmonized to water molecules adsorbed physically [19]. The absorption bands at 709 cm-1 and 590 cm^{-1} are produced by TiO_2, which are known to be the typical peak for Ti-O stretching vibrations [20,21]. In addition, the spectra of TiO_2 reveal all the dominant vibrational modes, showing acceptable affiliation with the literatures [19–21]. Also, new absorption peak at 445 cm^{-1} was appeared indicating F-Ti bond vibration. Meanwhile, Si-O-Ti stretching vibrations are noted at 912 cm^{-1}. Thus, it was confirmed that the impurities are well doped within the TiO_2 crystal lattice.

Morphology of prepared nanocomposites was determined using scanning electron microscope (SEM) and is illustrated in Fig. 6. The figure clearly shows that nanomaterials are demonstrating definite change in morphology and a trend for agglomeration of particle. Further it is showing an uneven particle distribution.

X-ray diffraction (XRD) is reported for the identification and characterization of crystalline solids. Every crystalline solid possesses its own unique XRD pattern that enables its identification. Fig. 7 shows the XRD patterns of as-prepared undoped TiO_2, Si-TiO_2 and F-TiO_2 nanomaterials. Presence of broad peaks in the pattern indicates the semi crystalline nature of as-prepared nanomaterials [22]. The diffraction lines obtained are well alligned with

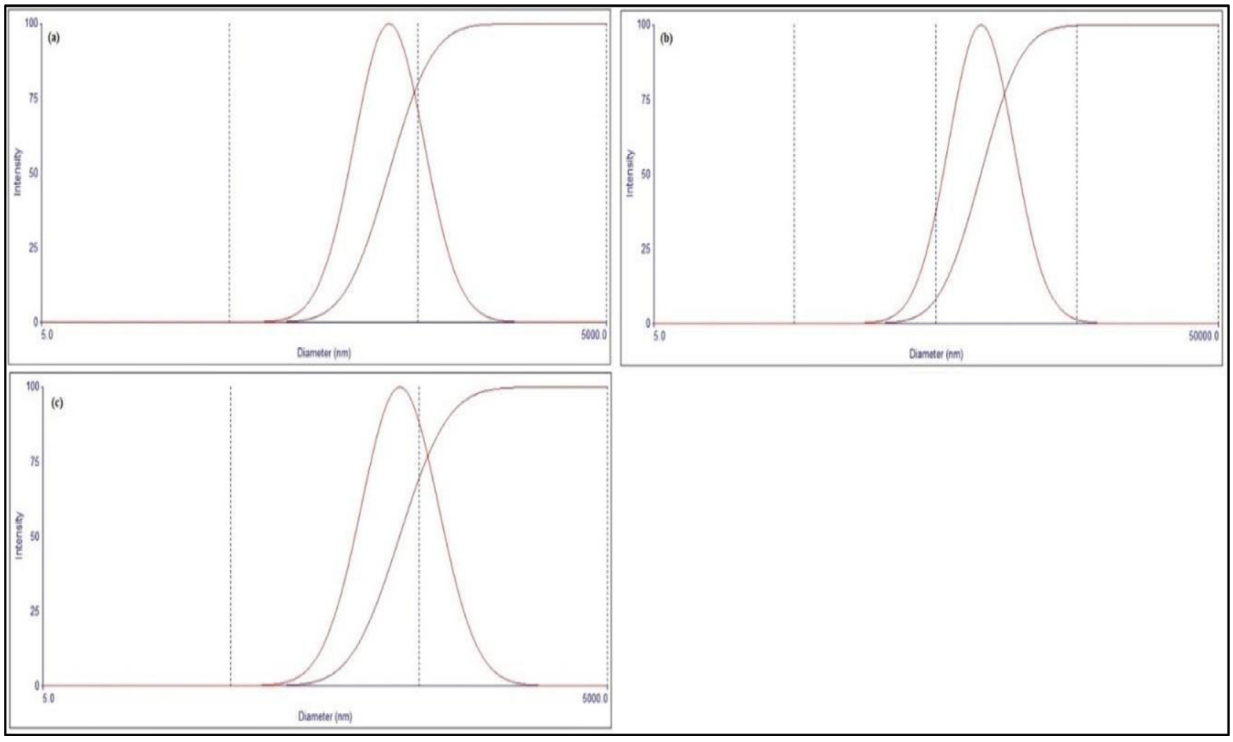

Fig. 3. The DLS analysis results of the prepared nanomaterials.

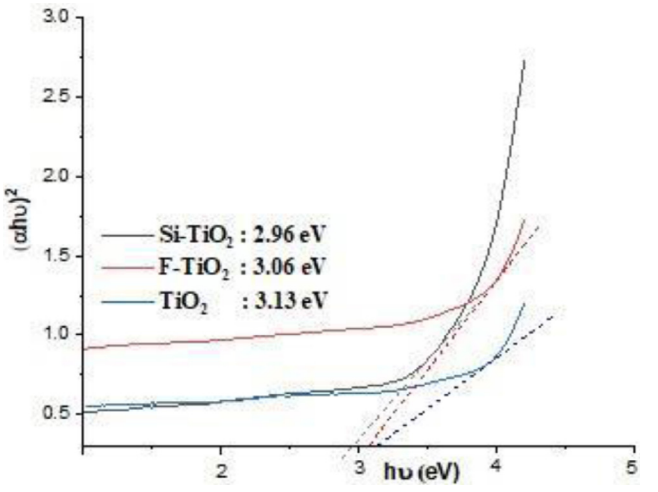

Fig. 4. Shifting of band-gap energy of Pure TiO_2, F-doped TiO_2, Si-doped TiO_2 nanoparticles.

the crystalline phase of anatase TiO_2 and are in good affiliation with reported pattern JCPDS 21-1275 of titanium dioxide. It was well-known that only anatase TiO_2 can be observed in the sample. The possible reason could be the presence of lower number of oxygen vacancies which may be due to higher amount of gaseous oxygen during the growth of particle [23]. Thus, it was concluded that as prepared samples are typical anatase titania crystal structure. (JCPDS 21-1275) with peaks at 2θ of 25.3, 37.9, 48.1, 54.02 and 55.13 corresponding to (101), (004), (200), (105) and (211) phases respectively [24,25].

3.2. Treatment efficiency with mechanism

3.2.1. Photocatalytic treatment of dye by pure TiO_2, Si-doped TiO_2 and F-doped TiO_2 coated on clay beads

Pure TiO_2, Si-doped TiO_2 and F-doped TiO_2 coated on clay beads are proved to be highly efficient, chemically inert and non-toxic during the process of dye degradation. To study the impelling role of dopants on the photocatalytic properties of the synthesized nanomaterials, a model dye like crystal violet and methyl orange was selected. To check the photodegradation efficiency the prepared samples were kept in the natural sunlight, LED light and in dark and were compared with blank samples simultaneously for a period of 5 hrs. Blank sample had 2.1% transmission initially for crystal violet and 0.3% for methyl orange. After the spectrophotometric studies, the degradation efficiencies (in %) were found to be as tabulated in Table 1. It was observed that all materials exhibit excellent photocatalytic activity under different light sources. Among all the samples which were kept in natural sunlight, Si-TiO_2 shows the higher degradation efficiency of more than 95% followed by F-TiO_2 and pure TiO_2 with a value of approximately 95% for both shown in Fig. 8(a) for crystal violet and 90% shown by all three prepared nanoparticles for methyl orange shown in Fig. 9(a). Samples kept in dark and after exposed to sunlight show good photodegradation for crystal violet with 90% and above 85% by Si-TiO_2, F-TiO_2 and pure TiO_2 respectively and above 95% for degradation of methyl orange shown by all the three prepared nanoperticles shown in Figs. 8(b) and 9(b) respectively. For the samples kept in LED light, Si-TiO_2 is showing the higher degradation efficiency of 85% shown by Si-TiO_2 followed by F-TiO_2 and pure TiO_2 with 80% and 78% respectively and around 90% of degradation is being observed in the methyl orange by all the prepared nanoparticles with a slightly change in difference shown in Figs. 8(c) and 9(c).

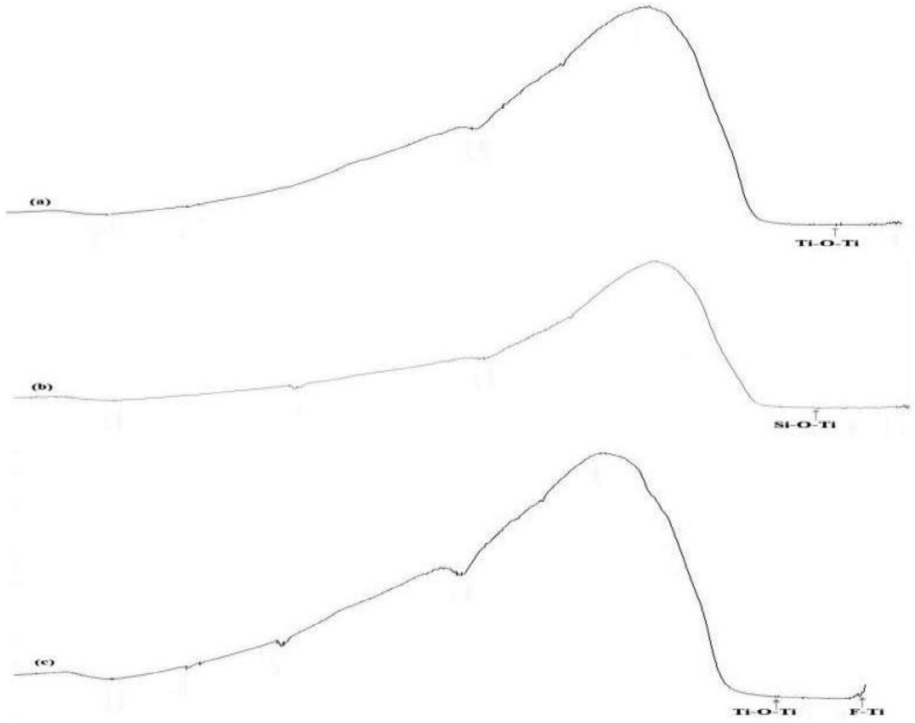

Fig. 5. FTIR Spectra of Pure TiO_2, F-doped TiO_2, Si-doped TiO_2 nanoparticles.

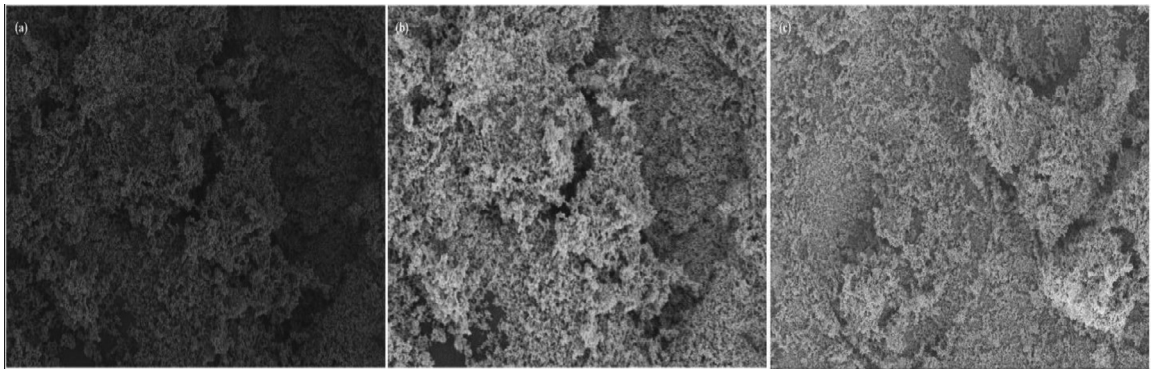

Fig. 6. SEM images of Pure TiO_2, F-doped TiO_2 and Si-doped TiO_2 nanoparticles.

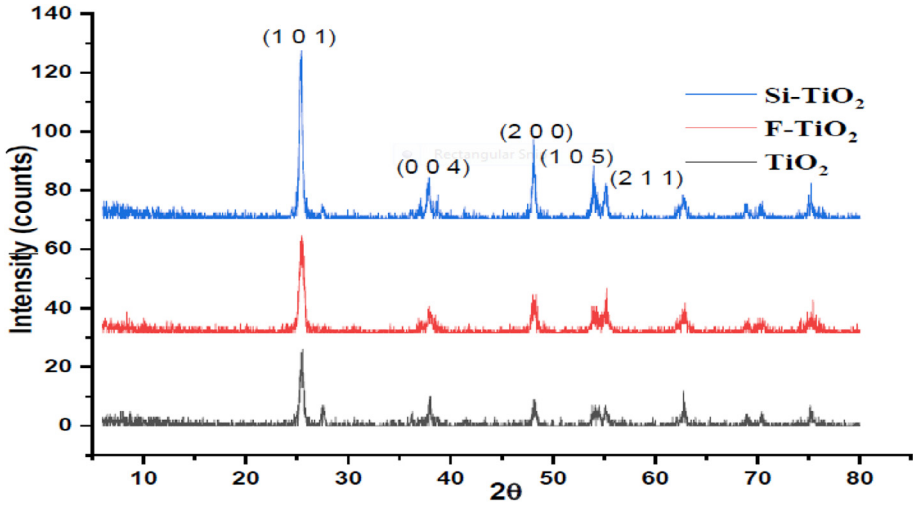

Fig. 7. XRD pattern of Si-doped TiO_2, F-doped TiO_2 and Pure TiO_2 nanoparticles.

Table 1
Degradation efficiencies of crystal violet, methyl orange, oil and grease and COD by nanomaterials.

Dye	Phase	Nanocomposites	Time (in hour)					
			1	2	3	4	5	6
Crystal Violet	Sunlight	TiO_2	91.28	92.01	94.81	95.04	95.73	
		F-TiO_2	92.57	93.26	93.85	94.15	96.18	
		Si-TiO_2	95.08	95.84	96.08	96.4	96.72	
	Dark + sunlight	TiO_2	25.0	36.36	75.58	84.67	89.55	
		F-TiO_2	55.31	58.82	83.06	90.09	91.1	
		Si-TiO_2	64.4	72.36	87.93	93.2	93.89	
	LED	TiO_2	63.79	66.66	76.4	79.0	83.2	
		F-TiO_2	70.83	76.4	80.0	82.35	86.95	
		Si-TiO_2	78.78	81.25	83.96	86.45	87.9	
Methyl Orange	Sunlight	TiO_2	66.66	87.5	96.63	97.58	98.33	
		F-TiO_2	81.25	90.63	97.58	98.76	98.96	
		Si-TiO_2	82.35	88.46	97.47	98.57	98.75	
	Dark + sunlight	TiO_2	33.33	66.66	96.9	97.32	98.23	
		F-TiO_2	72.72	78.57	97.34	98.62	98.93	
		Si-TiO_2	40	80	97.72	98.42	98.7	
	LED	TiO_2	40	87.5	91.89	94.23	96.05	
		F-TiO_2	66.66	77.85	92.69	98.88	99.07	
		Si-TiO_2	67.14	85	97.34	97.5	98.18	
Oil and grease	Sunlight	TiO_2		40.68		70.57		72.57
		F-TiO_2		58.27		69.48		71.91
		Si-TiO_2		69.42		70.038		72.97
	Dark + sunlight	TiO_2		26.05		34.24		40.58
		F-TiO_2		30.84		43.97		63.8
		Si-TiO_2		29.07		55.76		66.23
	LED	TiO_2		30.7		46.13		62.73
		F-TiO_2		43.97		49.7		66.74
		Si-TiO_2		47.78		61.95		75.51
COD	Sunlight	TiO_2		16.66		50		75
		F-TiO_2		33.33		65.66		83.3
		Si-TiO_2		35		67.66		85.3
	Dark + sunlight	TiO_2		15.3		45.2		74
		F-TiO_2		21.2		57.4		80.3
		Si-TiO_2		23.5		61.3		82.3
	LED	TiO_2		16.4		47.6		78.2
		F-TiO_2		31.4		59.8		83.5
		Si-TiO_2		34.3		64.5		85.1

The samples kept under dark conditions show a slightly slower degradation efficiency of dyes initially but later increase. The initial lag in degradation was due to the absence of light source. This provides evidence that the synthesized nanomaterials work efficiently under visible spectrum and are multifunctional in nature. There has been a significant rise in photocatalytic activity during the initial hours due to the synergic effect of adsorption and photoactivity of nanomaterials. There was no considerable increase in photoactivity after a particular period of time. This was mainly due to the agglomeration of dye particles around the nanomaterials where it gets saturated and reaches to equilibrium. Comparing the light sources, it was noted that nanomaterials work efficiently under visible light source compared with that of LED. While comparing the efficiency of nanomaterials in dye degradation, Si-TiO_2, F-TiO_2 and doped TiO_2 almost exhibit similar results. This can be attributed to the adsorption activity employed by clay particles in nanomaterials. Thus, it was evident that the as-prepared nanomaterials display excellent photocatalytic activity under visible spectrum of radiation. The similarity in degradation efficiencies for both the dye was because of the reduced band gap and the synergic effect of clay. Hence, we can say that the photodegradation of methyl orange was almost shows similarity with that of the degradation of crystal violet.

3.2.2. Photocatalytic degradation of organic pollutants in real-time wastewater

Degradation of Oil and Grease in the real-time wastewater effluents under various light sources was carried out using pure TiO_2, Si-TiO_2 and F-TiO_2 nanoparticles coated on clay beads and the initial content was found to be 0.7890 mg/L. The wastewater sample was collected from the municipal sewage from sewage treatment plant located in Mysore city. The samples were subjected to irradiation for upto 6 h and tested every 2 h once. Under natural light all the prepared nanomaterials exhibit similar degradation efficiency of 70% shown in Fig. 10(a). This could probably be due to the light intensity and photon intensity of natural light. Whereas the samples placed under dark conditions prior to exposure to natural light exhibits lower degradation efficiency 65%, 63% and 35% by Si-TiO_2, F-TiO_2 and pure TiO_2 respectively shown in Fig. 10(b). The plausible reason may be due to the adsorption of oil and grease onto the surface of nanomaterials which restrict the access of light for photoactivity. Under LED irradiation, Si-TiO_2 showed a significant dominance over F-TiO_2 and pure TiO_2 with an efficiency of more than 70% which may be due to the reduced band gap of the Si-TiO_2 depicted in the Fig. 10(c).

Together with the photodegradation of oil and grease one more important parameter was checked and that is COD which is an important parameter for wastewater identification. The initial COD was found to be 600 mg/L. After subjecting the waste water samples to photodegradation with a period of 6 h results were observed. The results were found to be similar in all the light sources among which Si-TiO_2 is showing efficiency around 90%, F-TiO_2 above 85% and pure TiO_2 of 75% shown in Fig. 11(a, b, c) which clearly illustrates that Si-TiO_2 is having dominant efficiency over F-TiO_2 and pure TiO_2. Degradation of oil and grease and COD was noted maximum under natural light compared to LED and was

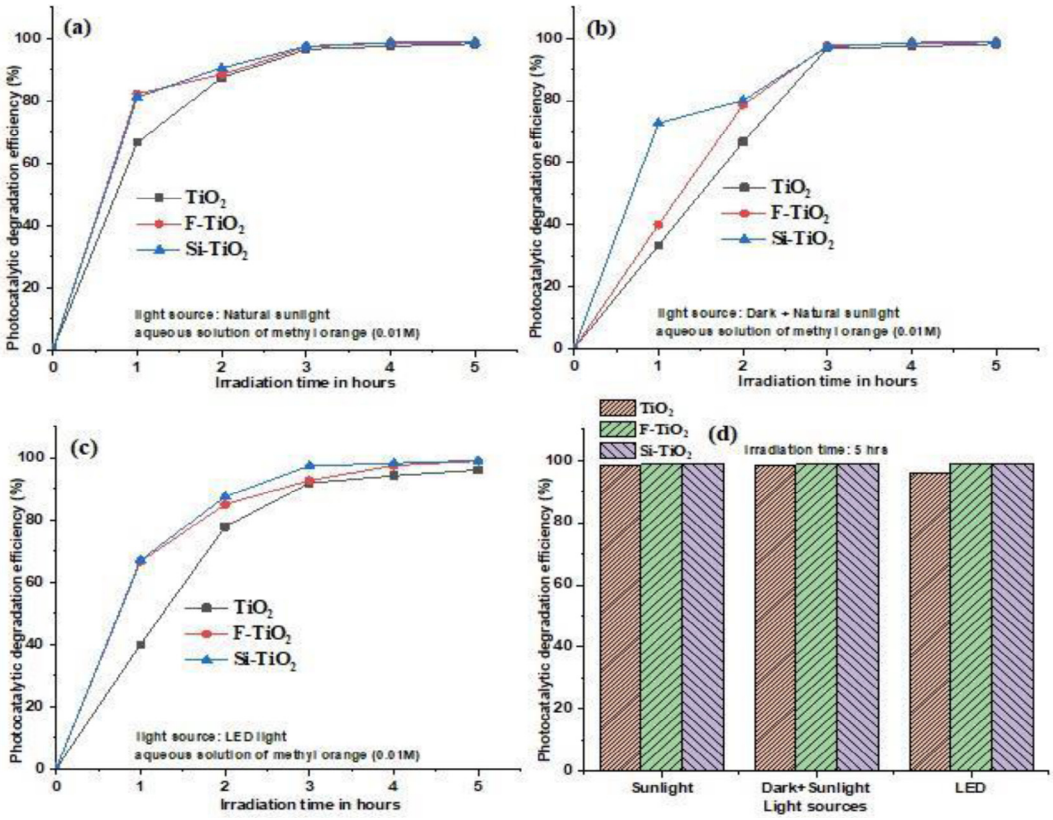

Fig. 8. Graphs illustrating the degradation efficiencies of CV by nanomaterials under different light sources.

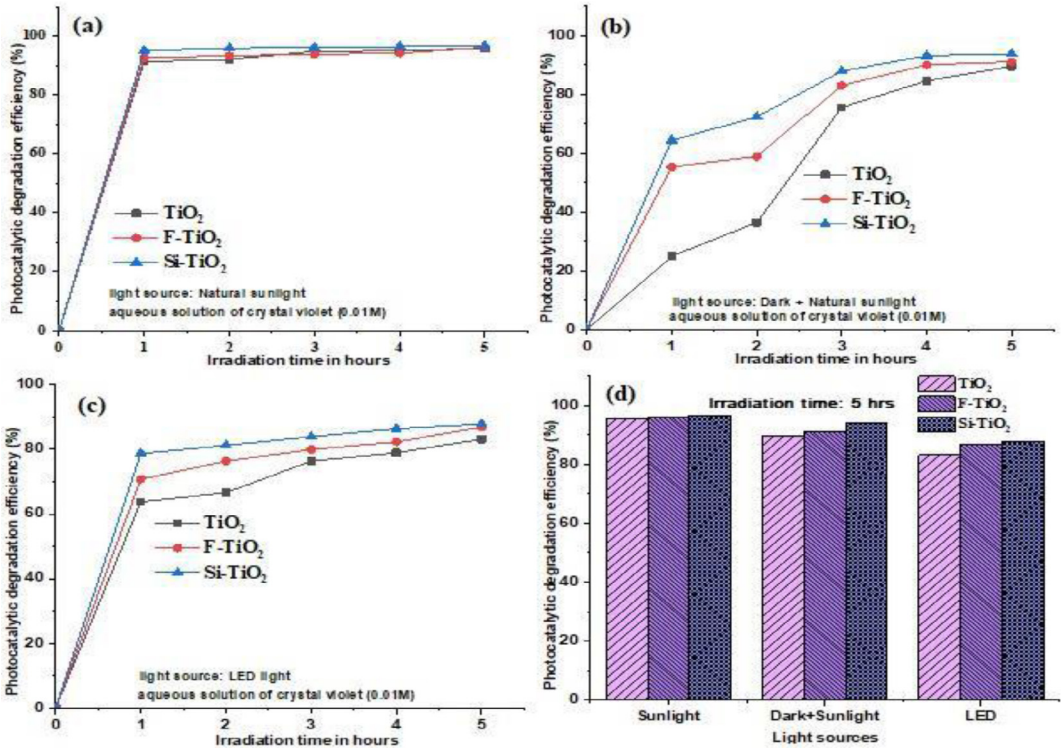

Fig. 9. Graphs illustrating the degradation efficiencies of MO dye by nanomaterials under different light sources.

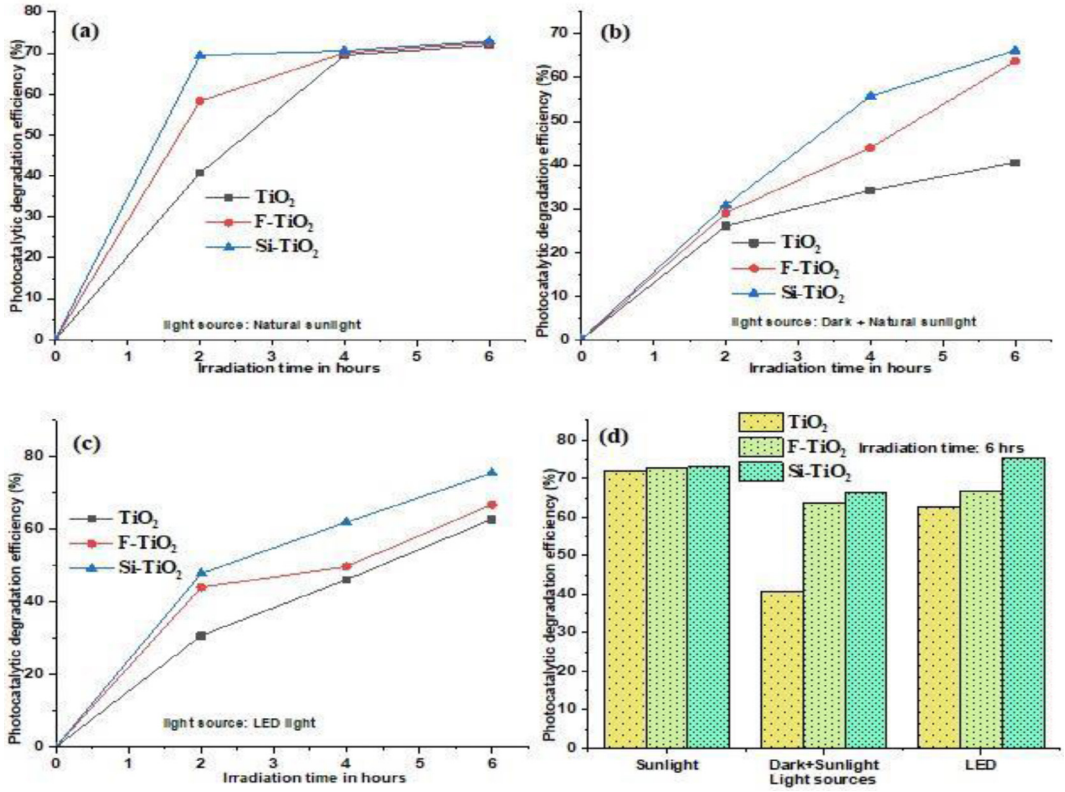

Fig. 10. Graphs illustrating the degradation efficiencies of oil and grease by nanomaterials under different light sources.

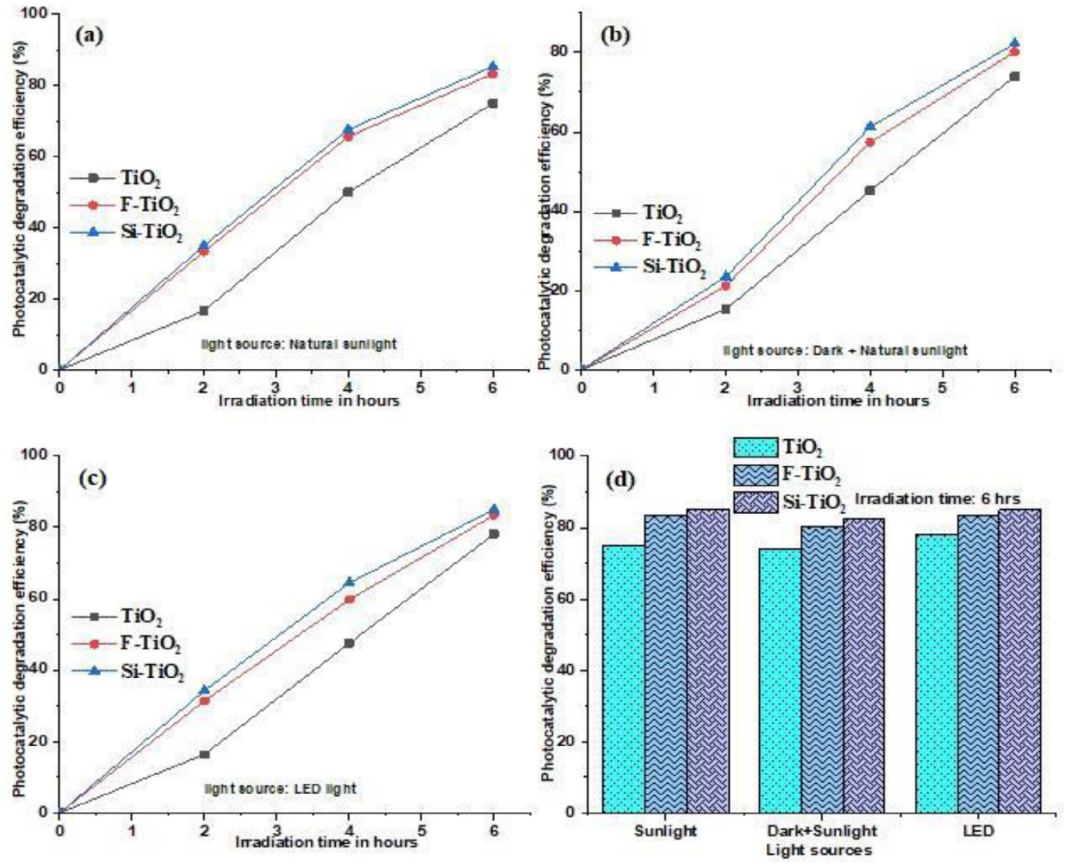

Fig. 11. Graphs illustrating the degradation efficiencies of COD by nanomaterials under different light sources.

attributed to the light intensity and photon energy which clearly indicates that synthesized materials exhibit a synergic effect in degrading organic pollutants and clay acts as an excellent adsorption material in enhancing the overall degradation efficiency of photocatalyst.

3.2.3. Advantages

On comparing the direct dispersion or other form of suspension of photocatalyst, floating photocatalyst shows an incisive advantage such as maximum potential use of light with enhanced photocatalyst reactivity [12,26] on the bead surface as it receives sufficient amount of dissolved oxygen and H2O present at the air-water contact surface [12,27–29] leads to enhanced oxidation efficiency resulting in efficient degradation of most of the organic contaminants present in water. Post-treatment separation process and recovery of floating beads easily by sieving is proved easy and cost-effective facilitating it for reusing for the next cycle [30–36]. Due to an exclusive structure of floating beads coated with nanoparticles provides several more advantage such as it reduces the loss and mass of photocatalyst coated on beads, rotation of floating beads on the surface either naturally by wind flow or by providing some kinetics, it provides an enough surface area in order to complete the photodegradation and prevent the interaction between the organic pollutants and photocatalysts for a longer duration which is the reason for decrease in photocatalytic reactivity [1].

4. Conclusions

This current research focuses on the preparation of visible-light responsive F-doped and Si-doped titanium dioxide photocatalytic nanomaterials to alter the band-gap energy of pure TiO_2 using sol–gel technique so as to enhance its excellent photocatalytic properties in the visible light region as its optimum efficiency is observed in the UV region. The entire experiment was conducted in a cost effective manner using relatively eco-friendly materials. Multifunctional coated pure TiO_2, Si-TiO_2 and F-TiO_2 were architecture fruitfully using clay and thermocol beads. Characterization experiments determined the structure and properties of these materials and further helped establish the activity of the nanomaterials in the visible light region. The nanomaterials were tested for their degradation properties with respect to pollutants such as dyes and oil and grease and were easily recovered from the samples. In all the tested parameters, i.e. dye degradation, oil and grease degradation and COD reduction, it was observed that the best results were obtained under natural sunlight (visible range) which is renewable energy. In most of the results obtained, Si-doped TiO_2 seemed superior over F-doped and pure (undoped) TiO_2 in its degradation efficiencies. Spherical form of beads ensures that in natural ambient conditions, without the aid of external kinetic energy, a simple gust of wind would provide the necessary friction for the spheres to rotate on their own and expose all the active sites containing the nanomaterials to the light source as well as to the pollutants present in the water. With further development and research in this field, it is possible to be implemented by every industry to treat effluents efficiently and reduce the load dumped into water bodies.

Declaration of Competing Interest

The authors declare that they have no known competing financial interests or personal relationships that could have appeared to influence the work reported in this paper.

Acknowledgement

The authors wish to thank the Department of Water and Health, JSS Academy of Higher Education and Research, Mysore for supporting other aspects of the work and ICNAN'19 for the opportunity to present the work.

References

[1] X. Zipeng, Z. Jiaqi, C. Jiayi, Y. Junwei, Z. Tianyu, K. Junyan, X. Ziyuan, W. Ning, Z. Wei, Appl. Catal. B: Environ. 225 (2018) 452–467.
[2] H.P. Shivaraju, G. Midhun, K.M. Anil Kumar, S. Pallavi, N. Pallavi, B. Shahmoradi, Appl. Water Sci. 7 (2017) 3937–3948.
[3] H.P. Shivaraju, N. Muzakkira, B. Shahmoradi, Int. J. Environ. Sci. Technol. 13 (2016) 2293–2302.
[4] H.P. Shivaraju, C.P. Sajan, T. Rungnapa, V. Kumar, C. Ranganathaiah, K. Byrappa, Mater. Res. Innov. 14 (2010) 80–86.
[5] Z. Aqun, F. Zhaoyang, L. Bin, S. Yanxia, L. Junwei, X. Yingxin, Nano Rep. 1 (2015) 24–28.
[6] H.P. Shivaraju, K. Byrappa, T.M.S. Vijay Kumar, C. Ranganathaiah, Bull. Catal. Soc. India. 9 (9) (2010) 37–50.
[7] M.M. Halmann, Photodegradation of Water Pollution, CRC Press, Boca Raton, 1996.
[8] K. Byrappa, A.K. Subramani, S. Ananda, K.M. Lokanatha Rai, C. Ranganathaiah, M. Yoshimura, Bull. Mater. Sci. 30 (2007) 37–41.
[9] J.S. Dalton, P.A. Janes, N.G. Jones, J.A. Nicholson, K.R. Hallam, G.C. Allen, Environ. Pollu. 120 (2002) 415–422.
[10] T.H. Lim, S.D. Kim, Chemi. Engine. Process. 44 (2005) 327.
[11] M. Darka, M. Stoja, R. Željko, Z. Irena, S. Zoran, R. Maja, Fibers Polym. 19 (2018) 1219–1227.
[12] S. Singh, H. Mahalingam, P.K. Singh, Appl. Catal. A: Gen. 462–463 (2013) 178–195.
[13] W. Xin, W. Wei, W. Xuejiang, Z. Jing, Z. Jianfu, G. Zaoli, Z. Lijie, Appl. Surf. Sci. 349 (2015) 264–271.
[14] M.E. Fabiyi, R.L. Skelton, J. Phochem. Photobiol. A: Chem. 132 (2000) 121–128.
[15] R.L. Pozzo, M.A. Baltanas, A.E. Cassano, Catal. Today. 39 (1997) 219–231.
[16] X. Wang, Z. Wu, Y. Wang, W. Wang, X. Wang, Y. Bu, J. Zhao, J. Hazard. Mater. 262 (2013) 16–24.
[17] H. Hun, R. Bai, Sep. Purif. Technol. 73 (2010) 142–150.
[18] S. Ankita, P.S. Bhanu, K.G. Arvind, Ind. J. Pure Appl. Phys. 52 (2014) 93–100.
[19] J. Xu, Y. Ao, D. Fu, C. Yuan, J. Phy. Chem. Solids. 69 (2008) 2366–2370.
[20] P. Praveen, G. Viruthagiri, S. Mugundan, N. Shanmugam, Spectrochim. Acta A. 120 (2013) 548–557.
[21] J. Wei, L. Zhao, S. Peng, J. Shi, Z. Liu, W. Wen, J. Sol-Gel Sci. Technol. 47 (2008) 311–315.
[22] C.L. Yeha, S.H. Yeh, H.K. Ma, Powder Technol. 145 (2004) 1–9.
[23] A.J. Rulison, P.F. Miquel, J.L. Katz, J. Mater. Res. 12 (1996) 3083–3089.
[24] M.A. Khan, M.S. Akhtar, O.-B. Yang, Sol Energy. 84 (2010) 2195–2201.
[25] S. Perumal, C. Gnana Sambandam, K. Monikanda Prabu, S. Ananthakumar, Int J Res Engg Tech. 3 (2014) 651–657.
[26] F. Magalhaes, F.C.C. Moura, R.C. Lago, Desalination 276 (2011) 266–271.
[27] L. Linze, L. Yi, X. Hang, Z. Wenlong, Sep. Purif. Technol. 52 (2015) 164–173.
[28] Z. Xing, J. Li, Q. Wang, W. Zhou, G. Tian, K. Pan, C. Tian, J. Zou, H. Fu, Eur. J. Inorg. Chem. 13 (2013) 2411–2417.
[29] G.Y. Yao, F. Chen, Sol. Energy. 79 (2005) 1–9.
[30] D. Suman, M. Hari, J. Chem. Technol. Biotechnol. 94 (2019) 2597–2608.
[31] S. Singh, P.K. Singh, H. Mahalingam, J. Mater. Environ. Sci. 6 (02015) 349–358.
[32] S. Singh, P.K. Singh, H. Mahalingam, Int. J. Environ. Res. 9 (2015) 535–544.
[33] X. Wang, X. Wang, W. Wang, J. Zhang, Z. Gu, L. Zhou, J. Zhao, RSC Adv. 5 (2015) 41385–41392.
[34] M. Długosz, J. Wa's, K. Szczubiałka, M. Nowakowska, J. Mater. Chem. A. 2 (2014) 6931–6938.
[35] H. Xue, Y. Jiang, K. Yuan, T. Yang, J. Hou, C. Cao, Sci. Rep. 6 (2016) 1–9.
[36] T. Leshuk, H. Krishnakumar, D. De Oliveira Livera, F. Gu, Water. 10 (2018) 1–8.